Journal of Advances and Scholarly Researches in Allied Education
Vol. 16, Issue No. 9, June-2019, ISSN 2230-7540

Comparative Study of Between Nanosecond Leser and Femtosecond Leser

Dr. Bipin Sinha*

Assistant Professor of Physics, Barsi College Pandygangout Nawada, Magadh University

Abstract – Micro- and Nano-machine researchers were especially interested in producing nanoparticles in liquid environments due to the straightforward method and the direct application of organic solvents with the ultra-short interaction of the laser pulse with materials. Furthermore, laser-produced colloidal nanoparticles are very pure — free of surfactants and reaction products or by products. This chapter examines the duration of the laser pulses in laser material processing of nanosecond, picosecond and femtosecond. Due to the special properties of laser pulse duration, which are short and ultra-short, in material processing, precise material processing and nanoparticles generation in liquid environments become more obvious laser.

Keywords: Nanoparticle Removal, Pulse Time, Nanosecond Reader, Femtosecond Reader Laser

----------X----------

INTRODUCTION

In addition to the laser wavelength, the main interaction parameters in pulsed laser applications are intensity G and laser pulse length. In laser handling two processes are dominant: ablation of material and plasma formation. These processes appear to be interconnected with plasma formation dynamics.

The generation and manipulation of nanoparticles were not only used for different laser-puls regimes (nanosecond, picosecond and femtoseconds). Different laser wavelengths were selected to reduce the size and morphology of nanoparticles. The study in this file focuses on the use for micro and nanomaterials of the various laser types and parameters. In addition to the production of new materials, researchers have used different types of lasers for accurate micro- and nano-machining. The generation of short and extremely short pulse lasers leads to laser processing with high precision. Lasers with pulse duration in the femtosecond to picosecond range show a significant quality change compared with nanosecond or long laser pulses for different materials. In addition, pulsed lasers are a promising alternative to chemical methods for manufacturing completely ligand-free, colloid nanoparticles for the production of nanoparticles in liquid environments.

FEMTOSECOND

In general, two different laser pulse time ranges are used for processing laser materials: long pulse time like the nanosecond pulse time, which generates a significant heat affected zone in the material since "this pulse time is longer than the heat of most metals." Short pulse time (picosecond laser) and ultra-short pulse time (femtosecond laser) produce better outcome in the high precision production of both micro and Nano machines. For precise laser material processing, the typical laser pulse duration is 10 ps or less. Appropriate laser pulse durations were shown between 10-100 ps for the micro-making of copper and stainless steel.

FEMTOSECOND LASERS

While LIBS is typically performed by laser Nano-seconds, recent research using femtosecond lasers (fs-LIBS) was performed [10–18]. The excitation pulse with ns-LIBS dissolves and vaporises the target material resulting in a plasma expansion of up to 8000 K. This hot plasma stimulates the species of atoms and ions, which then emit typical spectral lines. The relative strengths of the lines depend on local and plasma quenching temperatures. The plasma also produces a constant background spectrum in addition to the characteristic lines, which decreases when the plasma is cooler. Usually, a few micro seconds after plasma formation, Gated detectors are used to record low background fingerprint lines.

Unlike nanosecond pulses, femtosecond pulses are capable of stimulating radiative atomic and molecular states directly via multiphoton absorption processes due to their high intensity and short duration. This would lead directly after

excitation to unbalanced plasmas and corresponding emissions from spectral lines. The States responsible for the important emissions lines of the fingerprint could be selectively encouraged to improve sensitivity. Our paper aims to study the usefulness of femtosecond pulses to detect heavy elements by comparing the Uranium plasma spectrum obtained from nanosecond pulses to those stimulated by pulses of the femtosecond.

NANOSECOND

Zimmer proposed the laser-induced temperature distribution model for analytical solutions across internal solid-liquid interfaces (see figure 2a). It has been demonstrated that low laser pulse duration, sufficient interface absorption and high fluid absorption allow for high solid surface temperature. The temperature of the liquid environment is, as shown in Figure 2b, much higher than the temperature of the transparent solid material with nanosecond laser (20 ns).

NANOSECOND LASER

The duration of the laser pulse was shown to influence the ablation and penetration thresholds of both materials. Long pulse duration or longer laser pulse duration increases the threshold fluence and reduces the efficient energy penetration depth. Low-intensity laser-pulse interaction with the target material primarily heats the target surface by energy absorption, causing it to melt and vaporise. The goal vaporisation demands far more energy than melting. It should be pointed out. The electron and the gate (ion) temperatures are equal (Te = Ti = T) and the steam produced remains transparent for laser radiation. In other words, the electrons and the lattice temperatures remain in the same thermal equilibrium (Te = Ti = T) point as such, Eq. If the laser pulse lasts longer than the electron-phon energy transfer time. (5) Heat equation reduces:

$$C_i \frac{\partial T}{\partial t} = k_o \left(\frac{\partial^2 T}{\partial z^2} \right) + I_\alpha \alpha e^{-\alpha z} \qquad \text{E6}$$

Pulsed Laser Ablation

The quality of the processing outcome generally decreases by the accretion of the melt and thermally damaged work piece, thus increasing with shorter pulse duration in pulsed laser ablation. The efficiency of ablation also decreases, however. Single pulse boiling on micro-second pulses permits the production of a lot of holes within a short space of time. The quality and reproductivity of the holes is rather small, as there is a large amount of melt involved. Short and ultrashort pulses with adequate boiling strategies are applied if higher precision is required. During short pulse laser removal, only a small amount of melt happens, which results in increased accuracy. Laser pulses ultrashort allow even less thermal damage and near-melt free removal when working close to the ablation threshold. In the past, however, the ultrashort pulsed system medium laser power has not been sufficient to meet the industrial efficiency requirements. Only recently have first attempts been made in industrial production to apply ultrashort laser pulses. A study on short and ultrashort laser pulse ablation efficiency is presented below. Different pulsed laser systems have been used for this purpose, reflecting the state-of-the-art of available short and ultrashort beam sources.

In the range of laser pulses for femtoseconds and a few picoseconds, ultra short laser pulse duration can be used to produce high quality, exact materials. Extensive pulse time can interact only with electrons, but longer pulse time is interactive with lattice time. The heat conduction during the interaction of the ultra-short laser pulse with materials is limited. It should be mentioned. The material is thereby inflamed within a well-defined space, whereby mechanical and heat damage to the target area is minimised. Longer (nanosecond) pulse time radiation on materials, instead, causes the target material to be continually heated. By heat conduction, laser pulse energy is spread to an area outside the laser spot size which boils and evaporates the irradiated target. The boiling and evaporation of the target material leads to an unregulated melting layer. This problem may be due to imprecise machining or marking in the case of the nanosecond laser pulse duration.

There is existing research into laser-material interactions; however, it shows how various pulsed lasers, especially in nanotechnology, can be used to process materials. Furthermore, the laser ablation of nanoparticles in liquid environments is relevant and there are some evidence of the effects of laser pulse durations on nanoparticle ablation. Even more recent investigations on laser-material interactions and laser-generated nanoparticles tend to emphasise laser beam parameter and experimental configurations in order to produce small and well-distributed nanoparticles and the accuracy of material processing, with little emphasis on the optimal laser parameters for the processing of laser materials. Furthermore the conceptualisation of nanoparts' structure and phase produced by laser ablation in a liquid solution received little attention. In order to support and enhance the performance of laser material processing in nanotechnology, it is therefore crucial to understand the optimum pulse regime for these applications.

Laser-material interaction at different laser pulse durations

The laser removal of the materials begins with photon absorption, followed by heating and

photoionization by the laser beam of the subject area. Then, as solid fragments, vapours, liquid drops or a widening plasma pen, ablazed materials are released from the target area. The quantity and phase of the ablated material depend on the energy the target material absorbs. The laser beam energy is absorbed by free electrons from the material, followed by thermalisation inside the electrons and the transfer of energy to the bars after the laser material has interacted with shorts and low intensity by reverse braking. In the end, electron heat transfer to the target material will result in energy loss. When considered to be rapid thermalisation in the electron subsystem, the transmission of energy from the laser beam to the target material can be described by 1D and 2D diffusion models and when both grille and electron subsystems are characterised by their temperature (Ti grille and Te electro temperature)

$$C_e \frac{\partial T_e}{\partial t} = -\frac{\partial Q(z)}{\partial z} - \gamma (T_e - T_i) + S \qquad E_1$$

$$C_i \frac{\partial T_i}{\partial t} = \gamma (T_e - T_i) \qquad E_2$$

$$Q(z) = -k_e \left(\frac{\partial T_e}{\partial z} \right) \qquad E_3$$

$$S = I(t) A\alpha \, e^{-\alpha z} \qquad E_4$$

Where Q(z) is the heat flux along the z-axle perpendicular to the target surface material, S is the laser heat source, I(t) is the laser intensity as time dependent, A is the surface transmittance (A = 1 − R), R is the reflector of the objective material and 5-007 the absorbing coefficient of the target material. There are two non-linear differential shares. (1) and (2) are used to model te and ti cooling dynamics that take into account electron-phononon connexion and sample material thermal conductivity. Furthermore, these equations can be used to model time, te and ti the evolution of electron and gill temperatures. The following can be written: eqs, man. (1)–(4):

$$C_e \frac{\partial T_e}{\partial t} = k_e \left(\frac{\partial^2 T_e}{\partial z^2} \right) - C_i \frac{\partial T_i}{\partial t} + I(t) A\alpha e^{-\alpha z} \qquad E_5$$

COMPARISON OF NANO- AND FEMTOSECOND LASER

COMPUTING ALGORITHM

The differential problem (l)-(9) was solved by using the dynamic adaptation method of finite differential, which allows for the calculation of direct interphase boundary tracking and shock waves. As a result, up to 6 computer areas with seven borders, including six moving borders and a free right border in the air, are available. This includes two shock waves. Evaporation, overheated metastatic states and a wave of gas medium shock. These characteristics are typical for all time periods.

As we move between long and high pulses, however, not only changes phase transition dynamics and metastable states, but also the appearance of new phenomena — solid phase shocks and plasma formation on the vapour or gas medium. Low-term thermal plasma 5 can occur on the end of the pulse at 103 K < Tmax < 104 K. It is caused by dynamic forces of gas squeezing that are linked to the spread of strong vapour-provoked shock waves.

REVIEW OF LITERATURE

Andreas Tuennermann(2013) He was PhD in Physics in 1988 and 1992, respectively, from the University of Hanover. In 1998, as Professor and Director of the Institute of Applied Physics, he joined Friedrich-Schiller University in Jena, Germany. In 2003, he was applied optics and precisions engineer in Jena and appointed Director of the Fraunhofer Institute. He is known for his pioneering work in the field of fibre laser technology and the use of ultra-fast powered lasers for material processing.

Dumitru et al. (2012) After deep perforation with femtosecond pulses (5 > Voisey et al . (2001) a metallographer study of the steel and hard material hole profil was carried out with the aid of gas laser perforation. The use of auxiliary gases (oxygen / nitrogen) in laser drilling was found to have no mechanical or chemical effect on the thermal barrier covered (TBC) and uncoated super alloy.

Week et al. (2018) Studied the effects on the rate of boiling of femtosecond, picosecond and nanosecond pulses of copper workpieces. They found that the transition from vaporised material to the material was mostly melted from the morphology study in the wall at a pulse rate of 1-10 picoseconds. They said the hole in the air was perforated below 10 21 picoseconds, but rips were seen, but a greater quantity of material was melted at 10 picoseconds and above. Furthermore, it was found that a large amount of vaporised material for a puls length less than 10 picoseconds was identified when observing the surface of a laser drilled hole while less vaporised and more moulting material for more than 10 picoseconds had been observed.

Antonav et ai. (2014) Study the effect of pulse repetition and wavelength in the shot pulse area using second and third harmonic laser pulse radiation ImJ energy at 1030 and 775 nanometers, pulse width and variable repetition rate at 1-10 kHz. According to them, the absorption into the workpiece of laser radiation

and the pulse repetition rate at the boiling speed were responsible for the wavelength.

Ostermeyar et al. (2015) Percussion boiling on a 1 mm aluminium plate with 10 Nanosecond pulse duration of a Q-switched Nd-YAG laser. The optimal parameters for burr height and ablation rate have been examined.

Champbell et al. (2017) The interaction of ultrasonic laser pulses with aluminium was studied using a femosecond laser. According to them, ultra-shot pulses caused the materials to melt. With the use of the second harmonic and the vacuum processing 800 nanometer beam, the smelting was minimised and eliminated virtually. At the cost of the processing speed, the quality of the hole was improved and the second harmonic beam was most slow to apply. High drilling rates are the nanosecond component of the beam.

Gurauskis et al. (2018) On a Ni-YSZ cermet plate, the optimal ablation capacity was reported to be 6.9 GW / cm pulse irradiances, with a pulse frequency of 8–80 nanoseconds, with a wavelength of 1.06 pm.

Wang et al. (2013) The Ni-YSZ cermet plate conducted microboiling activities and indicated that the optimum ablation capacity was 6,9 GW / cm pulse irradiance at the pulse frequence of 8–80 nanoseconds with a wavelength of 1.06 pm.

OBJECTIVES OF THE STUDY

1. To study the comparative study between the nanosecond laser and the femtosecond laser

2. To study laser-material interaction at different durations of laser pulse

RESEARCH METHODOLOGY

RESEARCH DESIGN

BOUNDARY CONDITIONS

For the lea-hand fixed border we se

$$x = \Gamma_s : \; u = 0, \quad W_T = 0, \quad W_l = 0;$$

x = as much as = abs: 3 conservative laws are formulated at a melting point: mass preservation, dynamism and energy captured in the reference for melting / cristallisation framemoving with solid phase velocity $v_{sl} = v_{sl}^{*} - u_s$, where v_{sl}^{*} stands for front melting speed in the fixed ref-erense framework (lab) (crystallisation)

$$\rho_s v_{sl} = \rho_l (u_l - u_s - v_{sl}),$$

$$P_s + \rho_s v_{sl}^2 = p_l + \rho_l (u_l - u_s - v_{sl})^2,$$

$$W_1^T - W_s^T = \rho_s v_{sl} L_m^{ne},$$

where $W_s = -\lambda(T_s)\frac{\partial T_s}{\partial x}$, $W_l = -\lambda(T_l)\frac{\partial T_l}{\partial x}$, C_{ps}, C_{pl} is Ther mal capacity of solid and liquid phases, respectively,

$$L_m^{ne} = L_m + (C_{pl} - C_{ps})(T_s - T_m) + \frac{\rho_s + \rho_l}{\rho_s - \rho_l}\frac{(u_s - u_l)^2}{2}$$

The melting temperature is unbalanced. The Energy Conservation Act is complemented by the phenomenological state of temperature equality at inter-phase boundary representing Stefan 's different condition.

$$T_{sl} = T_s = T_l = T_m(P_s).$$

MATERIAL

Research was carried out on the aluminium target of approx . 30 μm of thickness at T0 = 273 K and P0 = 1 bar in air. Application was carried out. As thermal physical parameters, values were used for the solid and liquid aluminium phases. The temperature for balancing the melting is Tm, 0 = 933 K.

Approximated empiric relationship using the linear Tm(Ps) = (Tm, 0 + kPs), in which k = is the Tm(Ps) function.

TEMPERATURE

Tcr=8 to 103 K was assumed to be the critical aluminium temperature. The thermal conductivity / laser absorescence ratios were decreased exponentially from the temperature T = 0.85 T cr to a critical point level of 0.85 T = 0.01 T = 0.01 J/(K cm),5-007Ts()TlEx-Tlx-Lmnestоиии l–()22 vsl * ратаитии – vlv+) (= PllVlVl2+pv+ vvvlv+()2+=WlTwvvlvlvLvne, Wlvlvlvlv,= GAT)

DATA ANALYSIS

General Processes

Some of the phenomena are always present in condensed and gas media. For all regimes, the prevalence of phase transitions is common: melted and evaporated, superheated metastable and medium-shake waves. These characteristics are typical for all time periods. As we move between long and high pulses, however, not only changes phase transition dynamics and

metastable states, but also the appearance of new phenomena — solid phase shocks and plasma formation on the vapour or gas medium. Low-term thermal plasma 5 can occur on the end of the pulse at 103 K < Tmax < 104 K. It is caused by the gas dynamic squeeze forces, which are linked to the spread of a powerful steam powered shock wave.

Condensed Medium

The dynamics of phased transitions and their behaviour depending on the duration of the pulse are the most important function in applications (micromashining, bohring). Reducing the laser pulse duration at the same energy density involves a rise in the heating velocity, which results in increased speed vsl at t 0 of the front melting speed vsl ~ t–1/2. The actual front melting speed is however restricted. The hydrodynamics of the molten pool is one of the effective mechanisms of speed control[33]. The effect of melting temperature dependency Tm = Tm(PS) on the melting surface PS, which is determined by velocity vsl, may be determined in particular. The growth of vsl thus results in a higher PS pressure and the interphase temperature of Tsl = Tm(PS) and the increase of the Tm = Tm(PS) melting temperature limit the growth of vsl. With the reduction of the laser pulse time, the contribution of the overheated metastable States increases and the phase transition dynamics are defined in many respects.

A typical example of the ultrashort = 10 fs Laser Pulse solution spatial structure is shown when the shock waves form in the solid phase and the gas medium is 80 fs at Fig. 1. The time of front melting was defined by the temperature of the target surface heating at the Tm melting equilibrium temperature 0. When the target reached Tm, the first 0-thickness of the fluid phase of 0,02–0,20 nm was added. Mass absorption and volumetric mechanisms pass across x = sl interphase forms the highest undersurface temperature.

The air pressure starts convective evaporation from the surface at the moment the saturated vapour pressures are exceeded and a second phase is introduced. A further maximum subsuperior temperature is formed, Fig, affected by rapidly evaporating liquid, at a distance from the front evaporation. 1. The maximum temperature positions in solid and liquid phases are determined by the thermal conductivity ratio and phase front absorption coefficients. Vsl vlv is established since the relationship Fig. 2 The maximum solid phase temperature is considerably higher than the maximum liquid temperature.

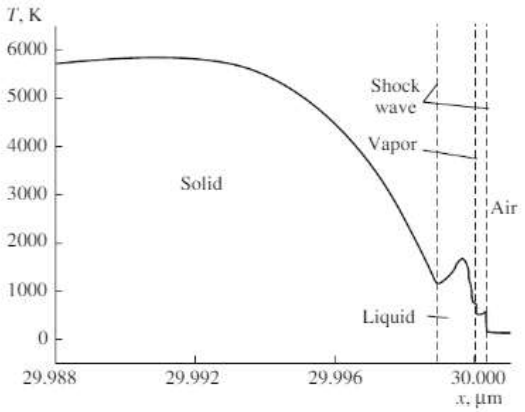

Fig. 1. Spatial temperature profile at t = 78.5 fs for laser pulse τ = 10 fs, G0 = 1014 W/cm2

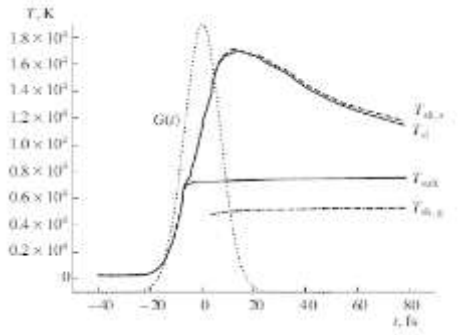

Fig. 2. Temporal profiles of temperature Tsl, Tsurf, Tsh, s, Tsh, g at the beginning and for a laser pulse τ = 10 fs, G0 = 1015 W/cm2

CONCLUSION

Our analysis shows that long and ultrashort pulses at the same energy density J differ fundamentally from mechanisms of transformation of laser energy. The solid phase (dizens degrees) is overheated smallly with amplifiers 2.5 times the evaporation time of the laser pulse. Most laser pulse energy is used in processes of melting and evaporation. The remainder is spent on the production of solid heat and shockwaves in the gas medium. The increasing proportion of laser pulse energy is used to overheat meta-stablely in the condenses and to produce shock waves for the solid phase and gas medium by shifting into an ultrashort laser pulse duration. The less energy is spent on the process of evaporation. So, if the pulse pulse time of the 10 ns pulse is not exceed 20 at 1 fs pulse time, the pulse pulse pulse duration is more than 30. The solid phase overheating range is Tmax / Tm0 = 8–10 and is close to critical temperature in the femtosecond range. In those situations it is highly likely that metastable states will decay from the spinods or that a new phase will be core, which corresponds to the shift from phase transformation to volumetrological mechanisms.

REFERENCES

1. Andreas Tuennermann (2013), UV Lasers: Effects and Applications in Materials Science (Cambridge Univ., Cambridge, 1996).
2. Dumitru et al. (2012), Math. Surv. Math.Industry 4, 85 (1994).
3. Week et al. (2018) e, Phys. Rev.B 61, 2643 (2000).
4. Antonav et ai. (2014). Electron. 25, 158 (1995) [Quantum Electron. 25,146 (1995)].
5. Wang et al. (2013) Laser Ablation. Principles and Applications, Ed. byJ. C. Miller (Springer, Berlin, 1994).
6. Gurauskis et al. (2018), Physical Processes atLaser Handling of Materials (Energoatomizdat, Moscow, 1985).
7. Antonav et ai. (2013) Proc. of the Institute of General Physics Academy of Sci-ences of the USSR, Ed. by (Nova Sci-ence Publ., New York, 1990), vol. 13.
8. Champbell et al. (2017) Appl. Surf.Sci. 253, 7744 (2007).
9. Dumitru et al. (2011), Appl. Surf. Sci.127–129, 983 (1998).
10. Gurauskis et al. (2018).Phys. 101, 24922 (2007).
11. Antonav et ai. (2015), Phys. Rev. E50, 4716 (1994).
12. Ostermeyar et al. (2015), Science 302, 1345 (2003)

Corresponding Author

Dr. Bipin Sinha*

Assistant Professor of Physics, Barsi College Pandygangout Nawada, Magadh University